Journal of Materials Chemistry B

Accepted Manuscript

ROYAL SOCIETY OF CHEMISTRY

www.rsc.org/materialsB

Journal of
Materials Chemistry B

RSCPublishing

ARTICLE

Distinct Optical and Kinetic Responses from *E*/*Z* Isomers of Caspase Probes with Aggregation-Induced Emission Characteristics†

Cite this: DOI: 10.1039/xoxxoooooox

Received ooth January 2014,
Accepted ooth January 2014

DOI: 10.1039/xoxxoooooox

www.rsc.org/

Jing Liang,‡[a] Haibin Shi,‡[a] Ryan T. K. Kwok,[b] Meng Gao,[c] Youyong Yuan,[a] Wenhua Zhang,[c] Ben Zhong Tang*[bd] and Bin Liu*[ac]

A dual-labeled probe for monitoring caspase activity was designed and synthesized based on a tetraphenylethene (TPE) fluorogen with aggregation-induced emission characteristics and a caspase-specific Asp-Glu-Val-Asp (DEVD) peptide. Two stereoisomers were furnished and successfully separated by HPLC. We demonstrated for the first time the effect of isomerization on the reaction kinetics between the probes and caspase. It was revealed that caspase can produce a much higher light-up ratio for *Z*-TPE-2DEVD probe, while its kinetics favor *E*-TPE-2DEVD due to enhanced probability of optimal binding between the two. Understanding the stereoisomers and their biological functions will open new opportunities for bioprobe design with optimized performance.

Introduction

Study of stereoisomers, which have the same molecular formula and different 3D atomic orientations, has great implications in enzymatic studies, drug discoveries, evaluation of drug efficacy and therapy development. The active sites of enzymes are usually relying on subtle geometric configurations of substrates, leading to distinctively different reactivities and products.[1] Many compounds are known to exhibit stereo-specific or stereo-dependent effects in biological functions or as therapeutic agents.[2] The development of probes with stereoisomers for biologically significant targets not only aids in stereochemistry studies, but also sheds light on the mechanism of ligand-target interaction for a wide range of clinical and diagnostic applications.[3]

Apoptosis, a self-programmed cell death process to eliminate redundant or senescent cells,[4] plays a critical role in regulation of biological functions, including normal cell turnover, immune response, wound healing, endocrine-dependent atrophy and development of individual organs.[5] Disruption of apoptosis can ultimately lead to a series of pathological conditions such as cancer and Alzheimer's disease.[6] The development of effective probes for study of apoptosis process is thus of clinical importance. Caspase, a group of cysteine-aspartic protease, plays a central role in initiation and execution of apoptosis through a cascade of activation or deactivation processes.[7] Among them, caspase-3 has been identified to be the most prominent player and has been well established as a biomarker for monitoring of apoptosis.[8] Common approaches for fabrication of caspase probes involve functionalization of a caspase-specific substrate such as Asp-Glu-Val-Asp (DEVD) peptide with a fluorophore or dual-functionalization with a pair of donor and acceptor.[9] The activity of caspase can be correlated with the change of fluorescence intensity or emission wavelength upon cleavage of the substrate. Although these approaches have been applied in both *in vitro* and *in vivo* apoptosis detection, limitations such as obvious fluorescence background or requirement of multiple steps remain an issue.

The discovery of a group of fluorogens with aggregation-induced emission (AIE) characteristics in 2001 has attracted intense research attention.[10] Unlike conventional fluorophores that experience fluorescence quenching at high concentration due to π-π stacking interaction,[11] fluorogens with AIE characteristics are almost non-fluorescent in solution state but emit strongly in aggregation state owing to their propeller-like structure. The AIE mechanism has been attributed to restriction of intramolecular rotations and blocking of non-radiative pathways in the aggregated form.[12] Through proper design of the AIE fluorogens, some fascinating probes have been developed for monitoring enzyme activity.[13] Among them, despite that tetraphenylethene (TPE) is capable of producing probes with *E*/*Z* isomers, no reports have discussed about the presence of isomeric probes and their individual interactions toward the target enzyme. Futhermore, there has been limited study on the different fluorescence behaviors of fluorophores on *E*/*Z* isomers.[14]

Our previous work has successfully demonstrated real-time monitoring of caspase-3/7 activity using an AIE probe which comprises a TPE unit and a caspase-3/7 specific DEVD substrate *via* a lysine linker.[15] In this contribution, to explore the effect of isomeric probes and their different interactions with caspase, we designed and synthesized a dual DEVD-labeled TPE probe (TPE-2DEVD) for *in vitro* monitoring of caspase-3 activity. As bisazido-functionalized TPE ($TPE\text{-}2N_3$), the precursor of the probe, exists in a mixture of two stereoisomeric forms due to unsymmetrical coupling of McMurry reaction. Previous endeavor has been successful in procuding pure stereoisomers of AIE fluorogens by hand-picking of individual crys-

tals based on their different morphologies.[16] However, such separation techniques require labor intensive procedures and cannot be applied for large-scale production. As enzymes are strictly specific and conformation sensitive to substrate,[17] The distinct spatial arrangements of DEVD arms between the two isomers are expected to induce different interactions between caspase and the probes. We hence, developed a strategy to produce pure isomeric AIE probes with the potential to scale up and explored their effectiveness as caspase-3 substrates for the first time. The probes in *E* and *Z* isomers are found to show different reactivities toward caspase-3 and display distinct light-up responses. The discovery is of practical importance in design and evaluation of effective bioprobes with optimized performance.

Experimental

Materials

4-Methylbenzophenone, zinc dust, *N*-bromosuccinimide (NBS), benzoyl peroxide (BPO), sodium azide, carbon tetrachloride, copper(II) sulfate, sodium ascorbate, *N,N*-diisopropylethylamine (DIEA), dimethyl sulfoxide (DMSO), trifluoroacetic acid (TFA), triisopropylsilane (TIS), piperazine-*N,N'*-bis(2-ethanesulfonic acid (PIPES), ethylenediaminetetraacetic acid (EDTA) and 3-[(3-cholamidopropyl)dimethylammonio]propanesulfonic acid (CHAPS) were all purchased from Sigma-Aldrich and used as received without further purification. All the solvents were purchased from Sigma-Aldrich and used as received without further purification, except for hexane and tetrahydrofuran, which were distilled from sodium benzophenoneketyl immediately prior to use. Titanium(IV) chloride was purchased from Merck. The Rink-amide resin, O-benzotriazole-N,N,N',N'-tetramethyl-uronium-hexafluoro-phosphate (HBTU), N-hydroxybenzotriazole (HOBt), Fmoc-protective amino acids and the alkyne-terminated DEVD peptide was purchased from GL Biochem Ltd. Bovine serum albumin (BSA), papain, lysozyme, pepsin, and trypsin were purchased from Sigma. Recombinant human caspase-3 and inhibitor Z-DEVD-FMK were purchased from R&D Systems and caspase-1, human recombinant, E. coli was purchased from Merk Millipore. Fetal bovine serum (FBS) and trypsin-EDTA solution were purchased from Gibco (Lige Technologies, AG, Switzerland). Staurosporine (STS) was purchased from Biovision. Milli-Q water was supplied by Milli-Q Plus System (Millipore Corporation, Breford, USA). MCF-7 breast cancer cell line was provided by American Type Culture Collection.

Characterization

UV-vis absorption spectra were taken on a Milton Ray Spectronic 3000 array spectrophotometer. Photoluminescence (PL) spectra were measured on a Perkin-Elmer LS 55 spectrofluorometer. All PL spectra were measured with an excitation wavelength of 320 nm. The cells were imaged by fluorescence microscope (Nikon A1 Confocal microscope). ^{1}H and ^{13}C NMR spectra were measured on a Bruker ARX 400 NMR spectrometer. High-resolution mass spectra (HRMS) were recorded on a Finnigan MAT TSQ 7000 Mass Spectrometer System operating in a MALDI-TOF mode. The HPLC profiles and ESI mass spectra were acquired using a Shimadzu IT-TOF. A 0.1% TFA/H_2O and 0.1% TFA/acetonitrile were used as eluents for all HPLC experiments. The flow rate was 0.6 mL/min for analytical HPLC and 3 mL/min for preparative HPLC.

Synthesis of 1,2-bis(4-methylphenyl)-1,2-diphenylethene (2). Into a nitrogen-filled 250 mL two-necked round-bottom flask were added 4-methylbenzophenone (5.89 g, 30 mmol), zinc dust (5.88 g, 90 mmol) and freshly distilled THF (100 mL). The solution was cooled to −78 °C in dry-ice/acetone bath. $TiCl_4$ (7.56 g, 90 mmol) was added dropwise. After refluxing overnight, the reaction mixture was cooled to room temperature. The mixture was poured into diluted hydrochloric acid and extracted with DCM several times. The organic layer was combined and dried over $MgSO_4$ and concentrated under reduced pressure. The crude product was further purified by a silica gel column using hexane as eluent to yield **2** as a white solid (5.25 g, 97% yield) (Scheme 1). ^{1}H NMR (400 MHz, $CDCl_3$) δ (TMS, ppm): 7.12–7.01 (m, 10H), 6.93–6.90 (m, 8H), 2.26 (s, 6H); ^{13}C NMR (100 MHz, $CDCl_3$) δ (TMS, ppm): 144.1, 140.9, 140.4, 135.8, 131.3, 131.1, 128.4, 127.5, 126.2, 21.2. HRMS (MALDI-TOF), *m/z* 360.1877 (M^+, calcd. 360.1878)

Synthesis of 1,2-bis[4-(bromomethyl)phenyl]-1,2-diphenylethene (3). Into a 100 mL round-bottom flask were added **2** (1.44 g, 4.0 mmol), freshly recrystallized NBS (1.57 g, 8.8 mmol), and catalytic amount of BPO (0.01 g) in 60 mL of carbon tetrachloride. The solution was refluxed for 10 h before it was cooled to room temperature. The solution was filtered and the filtrate was concentrated under reduced pressure. The crude product was purified by a silica gel column using hexane/chloroform (v/v = 4:1) as eluent to yield **3** as a white solid (1.08 g, 52% yield). ^{1}H NMR (400 MHz, $CDCl_3$) δ (TMS, ppm): 7.15–7.08 (m, 10H), 7.01–6.97 (m, 8H), 4.40 (s, 4H). ^{13}C NMR (100 MHz, $CDCl_3$) δ (TMS, ppm):144.3, 143.7, 141.3, 136.3, 132.1, 131.8, 128.9, 128.3, 127.2, 34.0. HRMS (MALDI-TOF), *m/z* 518.0305 (M^+, calcd. 518.0068).

Synthesis of 1,2-bis[4-(azidomethyl)phenyl]-1,2-diphenylethene (4). Into a 100 mL round-bottom flask were added **3** (0.78 g, 1.5 mmol) and sodium azide (0.39 g, 6.0 mmol) in 60 mL of DMSO. After stirring at room temperature overnight, the solution was poured into water and extracted with diethyl ether several times. The organic layer was combined and washed with water and brine, and then dried over $MgSO_4$. After filtration and solvent evaporation, the crude product was purified by a silica gel column using hexane/chloroform (v/v = 2/1) as eluent to give **4** as a white solid (0.54 g, 82% yield). The final product was characterized by NMR (Fig. S1) and HRMS (Fig. 1). ^{1}H NMR (400 MHz, $CDCl_3$) δ (TMS, ppm): 7.14–7.12 (m, 6H), 7.07–7.02 (m, 12H), 4.26 (s, 4H). ^{13}C NMR (100 MHz, $CDCl_3$) δ (TMS, ppm):144.4, 143.9, 141.4, 134.0, 132.4, 131.9, 128.5, 128.4, 128.3, 127.3, 55.2. HRMS (MALDI-TOF), *m/z* 442.1914 (M^+, calcd. 442.1906).

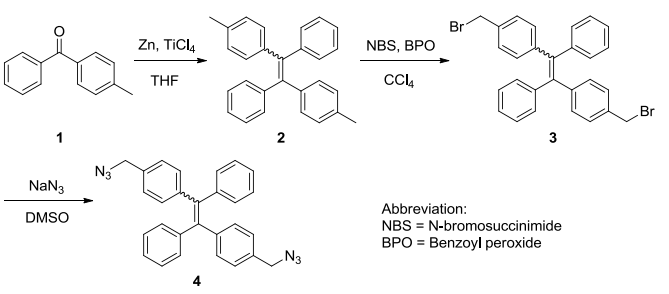

Scheme 1 The synthetic route to TPE-2N_3.

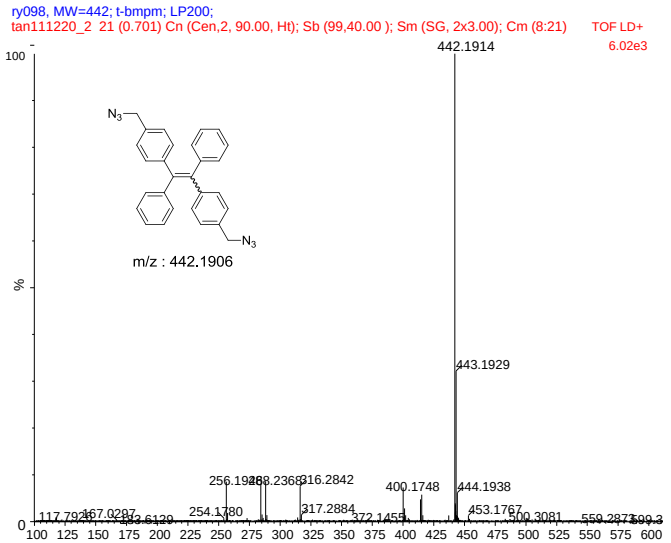

Fig. 1 High resolution mass spectrum of TPE-2N_3.

"Click" Synthesis of *E/Z*-TPE-2DEVD. DEVD-A (6.1 mg, 10 μmol) and **4** (TPE-2N_3) (2.2 mg, 5 μmol) were dissolved in 50 μL of DMSO. A mixture of DMSO/H_2O solution (v/v = 1/1; 0.5 mL) was subsequently added and the reaction was shaken for a few minutes to obtain a clear solution. The "click" reaction was initiated by sequential addition of catalytic amounts of sodium ascorbate (0.4 mg, 2.0 μmol) and $CuSO_4$ (1.6 mg, 1.0 μmol). The reaction was continued with shaking at room temperature for another 24 h. The final products were purified by prep-HPLC. HRMS (MALDI-TOF): *m/z* 1690.6659 ($[M+Na]^+$, calcd 1690.6872). The HPLC condition is: 20-100% B for 10 min, then 100% B for 2 min, 20% B for 5 min (Solvent A: 100% H_2O with 0.1% TFA; Solvent B: 100% CH_3CN with 0.1% TFA).

For *E*-TPE-2DEVD: ^{1}H NMR (400 MHz, DMSO-d_6, ppm) δ: 12.3 (br s, 6 H), 8.24 (d, *J* = 7.2 Hz, 2H), 8.18 (d, *J* = 7.8 Hz, 2H), 7.97 (t, *J* = 8.4 Hz, 4H), 7.80 (s, 2H), 7.68 (d, *J* = 8.4 Hz, 2H), 7.18 (s, 2H), 7.12–7.07 (m, 8H), 6.97–6.91 (m, 12H), 5.43 (s, 4H), 4.54–4.46 (m, 4H), 4.34–4.31 (m, 2H), 4.27–4.24 (m, 2H), 4.08 (t, *J* = 7.2 Hz, 2H), 3.08–3.04 (m, 2H), 2.90–2.86 (m, 2H), 2.66–2.64 (m, 4H), 2.53–2.44 (m, 4H), 2.22–2.17 (m, 4H), 1.92–1.88 (m, 4H), 1.81 (s, 6H), 1.74–1.72 (m, 2H), 0.74 (d, *J* = 6.6 Hz, 12H); ^{13}C NMR (100 MHz, DMSO-d_6, ppm) δ: 173.9, 172.1, 171.8, 171.6, 171.0, 170.9, 170.9, 170.1, 169.5, 143.1, 142.8, 142.6, 140.2, 134.2, 130.7, 130.4, 127.8, 126.9, 126.6, 123.1, 57.7, 52.4, 52.2, 52.0, 49.7, 49.6, 35.9, 35.6, 30.3, 29.9, 27.8, 26.9, 22.4, 19.0, 17.8.

For *Z*-TPE-2DEVD: ^{1}H NMR (400 MHz, DMSO-d_6, ppm) δ: 12.3 (br s, 6 H), 8.24 (d, *J* = 7.2 Hz, 2H), 8.18 (d, *J* = 7.6 Hz, 2H), 7.96 (t, *J* = 7.8 Hz, 4H), 7.83 (s, 2H), 7.69 (d, *J* = 8.4 Hz, 2H), 7.19 (s, 2H), 7.12–7.05 (m, 8H), 7.00–6.90 (m, 12H), 5.45 (s, 4H), 4.54–4.47 (m, 4H), 4.35–4.32 (m, 2H), 4.26–4.24 (m, 2H), 4.09 (t, *J* = 7.2 Hz, 2H), 3.08–3.05 (m, 2H), 2.91–2.87 (m, 2H), 2.67–2.61 (m, 4H), 2.53–2.44 (m, 4H), 2.22–2.17 (m, 4H), 1.93–1.88 (m, 4H), 1.81 (s, 6H), 1.74–1.72 (m, 2H), 0.75 (d, *J* = 6.6 Hz, 12H); ^{13}C NMR (100 MHz, DMSO-d_6, ppm) δ: 173.9, 172.1, 171.8, 171.6, 171.0, 170.9, 171.0, 170.0, 169.5, 143.1, 142.9, 142.6, 140.2, 134.3, 130.8, 130.5, 127.7, 127.0, 126.5, 123.2, 57.7, 52.4, 52.2, 52.0, 49.7, 49.5, 35.9, 35.6, 30.3, 29.9, 27.9, 26.9, 22.4, 19.0, 17.8.

Synthesis of *E/Z*-TPE-2A. The alkyl functionalized amino acid (**5**) was first synthesized using standard Fmoc strategy with rink amide resin as the solid support (Scheme 2). The resin (100 mg, loading ~0.5 mmol/g) was swelled in HPLC-grade DMF for 1 h at room temperature. Subsequently, Fmoc group was deprotected in piperidine/DMF (v/v = 1/4) for 2 h at room temperature. Following piperidine removal, the resin was washed extensively with DMF and DCM and dried thoroughly under high vacuum. Next, alkyne-functionalized amino acid was dissolved in dry DMF (1.5 mL) together with HBTU (4 equiv.), HOBt (4 equiv.) and DIEA (8 equiv.). The dry resin was then added and the resulting mixture was shaken at room temperature. After overnight reaction, the resin was filtered and washed thoroughly with DMF (3×), DCM (3×) and DMF (3×) until the filtrate became colorless. After drying thoroughly under high vacuum, the Fmoc group was removed under 20% piperidine in DMF. The resin was then treated with a mixture of 95% TFA, 2.5% triisopropylsilane (TIS) and 2.5% H_2O for 4 h at room temperature. Following prolonged concentration *in vacuum* until >80% of cleavage cocktail was removed, the resulting crude product was purified by prep-HPLC to afford compound **5**. *E/Z*-TPE-2A was then synthesized *via* the click chemistry of **5** and TPE-2N_3. The obtained **5** was dissolved in DMSO together with 1.2 equivalent (eq) of TPE-2N_3. An aqueous solution containing 0.2 eq of $CuSO_4$ and 0.4 eq of sodium ascorbate was added to the mixture to initiate the click reaction. The mixture was further shaken for 24 h and the products were purified by HPLC to yield *E/Z*-TPE-2A which were characterized by LC-MS. IT-TOF *m/z* $[M+H]^+$ calcd: 667.3179, found 667.2737. The HPLC condition is: 20-100% B for 10 min, then 100% B for 2 min, 20% B for 5 min (Solvent A: 100% H_2O with 0.1% TFA; Solvent B: 100% CH_3CN with 0.1% TFA).

General Procedure for Enzymatic Assay. 1 μL DMSO stock solutions of *Z/E*-TPE-2DEVD were diluted with caspase-3 assay buffer (50 mM PIPES, 100 mM NaCl, 1 mM EDTA, 0.1% w/v CHAPS, 25% w/v sucrose, pH = 7.2) to make 47 μL working solutions (10 μM). 3 μL of the recombinant caspase-3 (~0.05 μg/μL stock solution in assay buffer) was added into the above working solution. The reaction mixture was incubated at room temperature for 60 min and was then diluted to a total of 300 μL with deionized water for photoluminescence measurement. For inhibition study, caspase-3 was incubated with inhibitor *Z*-DEVD-FMK (10 μM) for 20 min prior to incubation with *Z/E*-TPE-2DEVD probes for another 60 min. The solution was excited at 320 nm, and the emission was collected from 360 to 600 nm.

Cell Culture. MCF-7 cell lines were provided by American Type

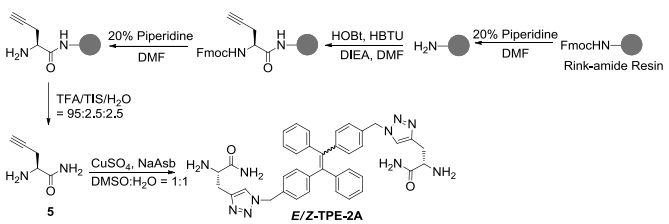

Scheme 2 Synthesis of cleaved products *E/Z*-TPE-2A.

Culture Collection. MCF-7 breast cancer cells were cultured in DMEM (Invitrogen, Carlsbad, CA) containing 10% heat-inactivated fetal bovine serum (FBS; Invitrogen), 100 U/mL penicillin and 100 μg/mL streptomycin (Thermo Scientific) and maintained in a humidified incubator at 37 ℃ with 5% CO_2. Before experiment, the cells were pre-cultured until confluence was reached.

Microscopy Imaging. MCF-7 cells were cultured in the chambers (LAB-TEK, Chambered Coverglass System) at 37 °C. After 80% confluence, the adherent cells were washed twice with 1 × PBS buffer. The *Z*- or *E*-TPE-2DEVD solution (10 μM, 0.3 mL) was then added to the chamber. After incubation for 2 h at 37 °C, the cells were washed once with 1 × PBS buffer, and treated with 3 μM staurosporine, for 1 h. The cells were washed one time with 1 × PBS buffer. The imaging was then done with fluorescence microscope (Nikon) equipped with DAPI filters. For colocalization with active caspase-3 antibody, the cells were first fixed for 15 min with 3.7% formaldehyde in 1 × PBS at room temperature, washed twice with cold 1 × PBS again, and permeabilized with 0.1% Triton X-100 in 1 × PBS for 10 min. The cells were then blocked with 2% BSA in 1 × PBS for 30 min and washed twice with 1 × PBS. The cells were subsequently incubated with a mixture of anti-caspase-3 antibody/1 × PBS (v/v = 1:99) for 1 h at room temperature, washed once with 1 × PBS buffer, and then incubated with mouse anti-rabbit IgG-TR (0.8 μg mL−1) in 1× PBS for 1 h, following by washing with 1 × PBS again. The imaging was acquired with a confocal microscope equipped with DAPI, FITC, and Texas Red filters.

Molecular Modelling. To explore the binding mode between TPE-2DEVD and caspase-3, we carried out molecular-docking studies with the X-ray crystal structure of caspase-3 (PDB ID 2H5I) using AutoDock Vina software. Caspase-3 structure was obtained from the PDB databank. Explicit hydrogen atoms were added and all water molecules were removed. The peptide ligand was also removed and the protein structure was processed using AutoDock Tools. The compounds were prepared for docking using AutoDock Tools to assign AD4 atom types, calculate Gasteiger charges, and set all rotatable bonds as active torsions. The ligand was docked into the protein using AutoDock Vina (version 1.11, The Scripps Research Institute). The exhaustiveness parameter was set to 100 (default = 8, linear scale); all other default settings were used. The macromolecule molecular surface and secondary structure were displayed by PyMol (version 0.99, DeLano Scientific LLC).

Results and discussion

TPE-2DEVD was synthesized by a copper catalyzed "click" reaction between TPE-$2N_3$[18] (Scheme 1), and an alkyne-bearing DEVD peptide (DEVD-A) in a DMSO/water mixture (Scheme 3). An isomeric mixture of *E*-TPE-2DEVD and *Z*-TPE-2DEVD was afforded in 90% yield. The introduction of DEVD peptides into the TPE core made it possible to separate the two isomers easily using HPLC due to the difference in hydrophobicity and size. After HPLC separation, two isomers were then characterized by NMR (Fig. S2) and high resolution mass spectra (HRMS). In order to confirm the respective isomeric structures of the two isomers, we tried to grow single crystals using the separated TPE-2DEVD products but failed. As small molecules are much more prone to crystalize,[16] it is possible to determine the molecular structures of their respective precursors TPE-$2N_3$ by growing crystals. HPLC was employed to separate *E*/*Z*-TPE-$2N_3$ into individual isomers though it requires much more rigorous

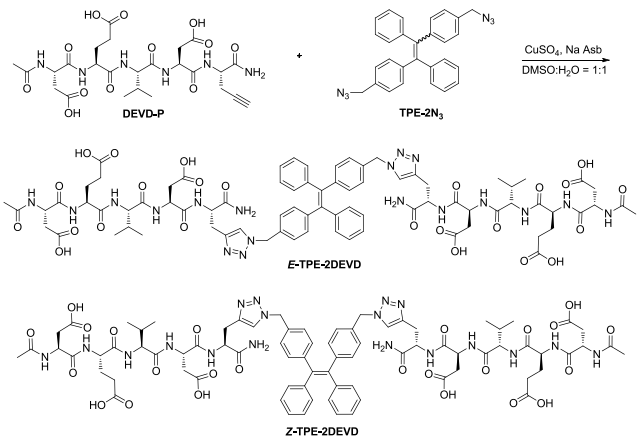

Scheme 3 "Click" synthesis of *E*- and *Z*-TPE-2DEVD.

separation conditions (due to very similar retention time between *E*- and *Z*-TPE-$2N_3$) to achieve efficient separation as compared to their peptide-functionalized counterparts. Their molecular structures were characterized by NMR (Fig. S3). The first elusion product of TPE-$2N_3$ was allowed to grow single crystals. The X-ray diffraction (XRD) crystallography results reveal the product to be *E* stereoisomer of TPE-$2N_3$ (Fig. S4). CCDC 968785 contains the supplementary crystallographic data for this paper.[19] Using the pure *E*-TPE-$2N_3$ as the starting material, only *E*-TPE-2DEVD was synthesized and purified by HPLC and characterized by NMR (Fig. S5). Both the retention time and NMR spectrum match well with that of the first eluted product of TPE-2DEVD synthesized initially (Fig. 2), proving that the first eluted TPE-2DEVD probe is *E* isomer and the latter eluent is *Z* isomer.

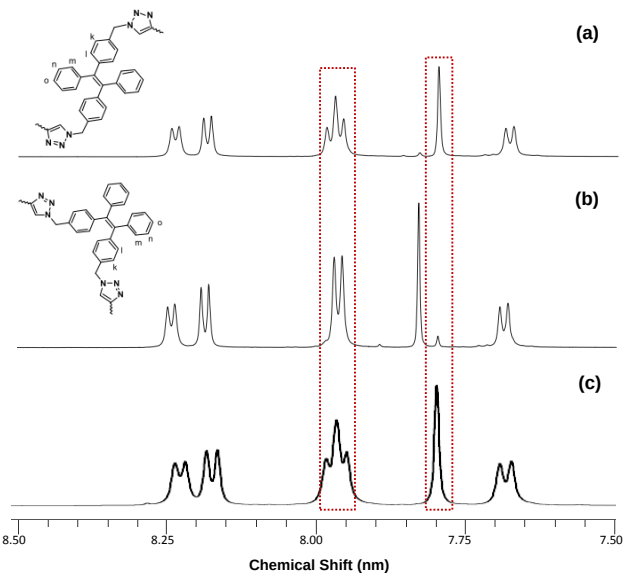

Fig. 2 Enlarged ^{1}H NMR spectra (7.50–8.50 nm) of (a) *E*-TPE-2DEVD in Fig. S3A and (b) *Z*-TPE-2DEVD in Fig. S3C and (c) *E*-TPE-2DEVD in Fig. S6A.

The UV-vis absorption spectra of *E*-TPE-2DEVD and *Z*-TPE-2DEVD in DMSO/water (v/v = 1/199) are shown in Fig. S6. Both isomers have a similar absorption profile with an obvious absorbance in 270–370 nm range. To investigate whether both *E*- and *Z*-TPE-2DEVD are AIE-active and responsive to caspase-3, we measured their fluorescence changes with and without treatment of recombinant caspase-3. As can be seen from photoluminescence (PL) spectra shown in Fig. 3A, both *E*-TPE-2DEVD and *Z*-TPE-2DEVD show no detectable fluorescence in a mixture of DMSO/PIPES buffer (v/v = 1/199), due to their good solubility in water. However, obvious fluorescence signals are recorded for both probes upon treatment with caspase-3 for 30 min. In the presence of a well-known, irreversible caspase-3 inhibitor, Z-DEVD-FMK, the fluorescence intensities of the probe solutions are suppressed due to inhibition of caspase-3, indicating the specific reaction between the probes and caspase-3. The enhanced fluorescence of the probes is attributed to the aggregation of cleavage residue, *E*-TPE-2A or *Z*-TPE-2A (Scheme 4), which is witnessed by laser light scattering (LLS) measurements, showing average mean particle sizes of 278.1 ± 6.5 and 266.7 ± 4.5 nm, respectively. It is also important to note that the fluorescence generated from cleavage of *Z*-TPE-2DEVD is apparently higher than that of *E*-TPE-2DEVD, which should be associated with the different fluorescent properties for the released *E*/*Z* -TPE-2A residues in aqueous media as discussed later.

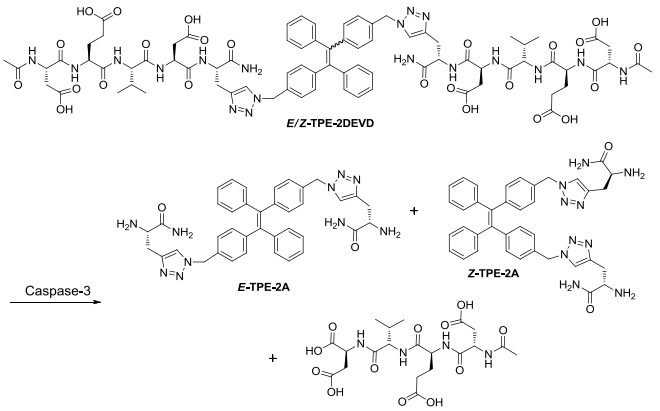

Scheme 4 The catalytic cleavage of TPE-2DEVD by caspase-3.

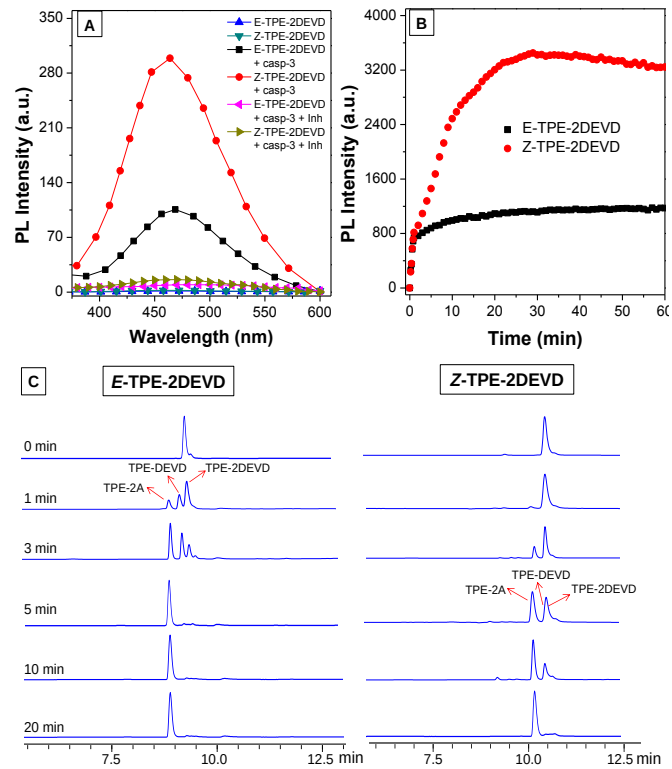

Fig. 3 (A) PL spectra of *E*- and *Z*-TPE-2DEVD before and after incubation with caspase-3 (casp-3) in the presence and absence of inhibitor (inh) *Z*-DEVD-FMK in DMSO/PIPES buffer (v/v = 1/199). (B) Time-dependent PL spectra of *E*- and *Z*-TPE-2DEVD upon addition of caspase-3 from 0 to 60 min. [*E*-TPE-2DEVD] = [*Z*-TPE-2DEVD] = [*Z*-DEVD-FMK] = 10 μM, [caspase-3] = 3 μg mL^{-1}, λ_{ex} = 320 nm. (C) Hydrolysis of *E*- and *Z*-TPE-2DEVD by caspase-3 monitored by reverse phase HPLC.

To investigate the kinetic property of the enzyme, both 2DEVD and *Z*-TPE-2DEVD were incubated with recombinant caspase-3 at 37 ℃, and the changes in fluorescence were monitored over time. As shown in Fig. 3B, both probes show gradually increasing fluorescence intensity over time. However, the fluorescence intensity of *E*-TPE-2DEVD reaches equilibrium within ~5 min, much faster than its Z-counterpart (~20 min). This indicates that the enzyme interacts with *E*-TPE-2DEVD more efficiently that leads to accelerated reaction rate. To reveal the structure-property relationship of the probes and the residues, we monitored the cleavage process of both probes using reverse phase HPLC-MS spectra over time. As shown in Fig. 3C, both probes were gradually hydrolyzed to the corresponding form of TPE-2A upon treatment with caspase-3. *Z*-TPE-2DEVD was cleaved over 20 min, while the same amount of *E*-TPE-2DEVD was completely hydrolyzed in 5 min, which is in agreement with the results of Fig. 3B. This indeed suggests that *E*-TPE-2DEVD is more effective for caspase-3 interaction and the difference in spatial arrangement between the probe and enzyme does have an impact on reaction kinetics. In addition, the retention time for *Z*-TPE-2A in the reverse phase HPLC spectra is 10.1 min, while that for *E*-TPE-2A is 8.9 min, which demonstrates that *Z*-TPE-2A is more hydrophobic than *E*-TPE-2A, taking into consideration of faster elution of molecules with smaller effective size (*Z*-TPE-2A). In order to further investigate the fluorescence properties of cleaved product *E*- and *Z*-TPE-2A, both compounds were synthesized by solid-phase synthetic method shown in Scheme 2 and characterized by LC-MS. The fluorescent intensities of *E*- and Z-TPE-2A in PIPES buffer were subsequently measured by PL spectrometer and they displayed around 258- and 123-fold higher fluorescence than probes alone, significantly improved as compared to DEVDK-TPE probe. The quantum yields of *Z*-TPE-2A and *E*-TPE-2A in 1 × PBS are 0.11 and 0.05 using quinoline sulfate as standard, respectively (Table 1).

We next performed the enzymatic assays for *Z*-TPE-2DEVD with different concentrations of caspase-3 ranging from 0 to 200 nM after 1 h incubation. Fig. 4A shows the variation in the PL spectra of the assays. With the increasing concentrations of caspase-3, the PL intensities gradually increase due to the increased amount of *Z*-TPE-2A released. The PL intensities of the probe at λ_{em} = 460 nm were

Table 1 Photophysical properties of quinoline sulfate, TPE-2N_3, *Z*-TPE-2A, *E*-TPE-2A and *E*/*Z*-TPE-2DEVD in 1 × PBS.

Samples	λ_{ex} [a]	λ_{em} [b]	Φ [c]
Quinoline sulfate	346	450	0.55
TPE-2N_3 [d]	320	490	0.24
Z-TPE-2A	320	470	0.11
E-TPE-2A	320	470	0.05
E/*Z*-TPE-2DEVD	320	470	0.0005

[a] λ_{ex} is excitation maxima; [b] λ_{em} is emission maxima; [c] Φ is quantum yield for 10 μM compound in 1 × PBS which is determined using quinoline sulfate as the standard; [d] isomericmixture of *E* and *Z* forms.

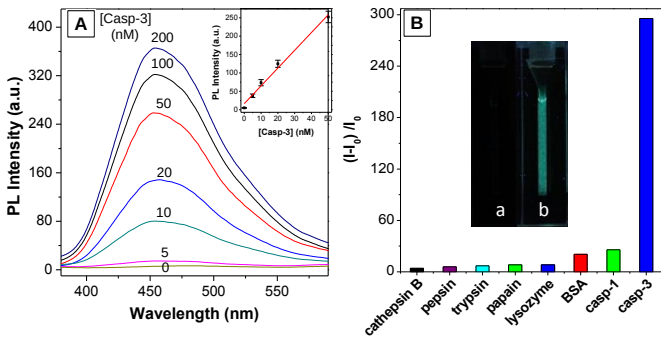

Fig. 4 (A) PL spectra of *Z*-TPE-2DEVD in the presence of different amounts of caspase-3 (casp-3, 0–200 nM). The inset shows the linear detection range of 0–50 nM caspase-3. (B) Plot of $(I-I_0)/I_0$ versus different proteins, where I and I_0 are the PL intensities at protein concentrations of 100 and 0 nM, respectively. [*Z*-TPE-2DEVD] = 10 μM. λ_{ex} = 320 nm. The inset shows the photographs of *Z*-TPE-2DEVD in the presence of cathepsin B (a) and caspase-3 (b) at 100 nM, respectively upon UV light illumination.

plotted against the concentrations of caspase-3 (Fig. S5) and the linear quantification range is shown in the inset of Fig. 5A. The limit of detection (LOD) of caspase-3 by the probe *Z*-TPE-2DEVD was evaluated to be 0.68 nM based on the 3 times standard deviation (3σ) method. To further investigate the probe selectivity, *Z*-TPE-2DEVD was treated with different proteins, such as cathepsin B, pepsin, trypsin, papain, lysozyme, BSA, as well as caspase-1 under identical conditions. As shown in Fig. 4B, caspase-3 displays apparent higher fluorescence change than the other seven proteins. This substantiates that *Z*-TPE-2DEVD is indeed a specific probe for caspase-3.

To gain insight into the binding mode of E-TPE-2DEVD and Z-TPE-2DEVD with caspase-3, we carried out molecular-docking studies with the X-ray crystal structure of caspase-3 (PDB ID 2H5I) using Autodock Vina software. The software generated results with the most optimal binding models which were all trans (*E*) form probes (Fig.5 and Fig. S8), indicating that *E*-TPE-2DEVD molecule binds well in the active site of caspase-3. Additionally, one of DEVD peptides in *E*-TPE-2DEVD overlays very well with DEVD-

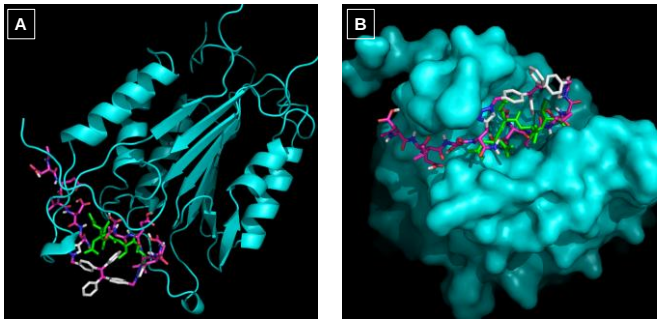

Fig. 5 Molecular docking of *E*-TPE-2DEVD and inhibitor DEVD-CHO in the active site of caspase-3. Caspase-3 is shown in sky blue. *E*-TPE-2DEVD is shown in multiple colors. DEVD-CHO is shown in green. (A) Overlay structures of *E*-TPE-2DEVD and DEVD-CHO binding to the active site pocket of caspase-3. (B) Superimposition of *E*-TPE-2DEVD bound to caspase-3.

CHO, a well-known caspase-3 inhibitor, which further demonstrates that *E*-TPE-2DEVD is the better binding substrate for caspase-3 to favor faster hydrolysis.

To further explore the potential of the probe for live-cell imaging of caspase-3 activation, confocal laser scanning microscopy (CLSM) was used to image the normal and apoptotic MCF-7 cells which were treated with *E*-TPE-2DEVD and *Z*-TPE-2DEVD, respectively. As shown in Fig. 6, the normal and un-induced cells show an extremely low fluorescence signal, indicative of little or no caspase-3 activity (Fig. 6A and 6E). In a sharp contrast, obvious fluorescence signals are collected from the cells treated by staurosporine (STS), a commonly used apoptosis inducer (Fig. 6C and 6G). The fluorescence signal of *Z*-TPE-2DEVD is evidently higher than that of *E*-TPE-2DEVD, which is consistent with their fluorescent characters shown earlier in Fig. 3. In addition, excellent overlap is observed between the fluorescence images of the probe and immunofluorescence signals generated from anti- caspase-3 primary antibody and a Texas Red-labeled secondary antibody (Fig. 7). The signal can be

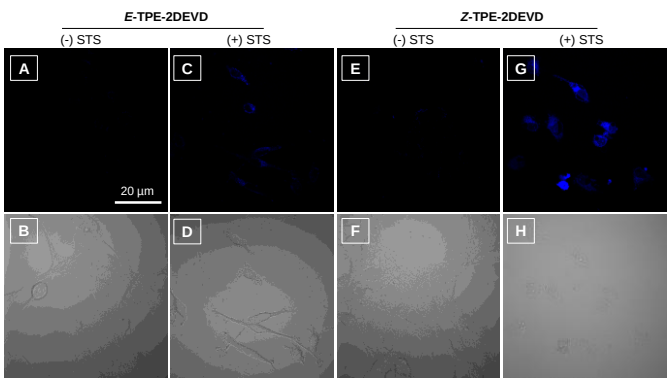

Fig. 6 CLSM images of normal MCF-7 cells treated with (A, B) *E*-TPE-2DEVD and (E, F) *Z*-TPE-2DEVD, apoptotic MCF-7 cells treated with (C, D) *E*-TPE-2DEVD and (G, H) *Z*-TPE-2DEVD. [*E*-TPE-2DEVD] = [*Z*-TPE-2DEVD] = 10 μM. Staurosporine (STS, 3 μM) was used to induce cell apoptosis. The images were acquired with a DAPI filter. The scale bar of 20 μm is applied to all images.

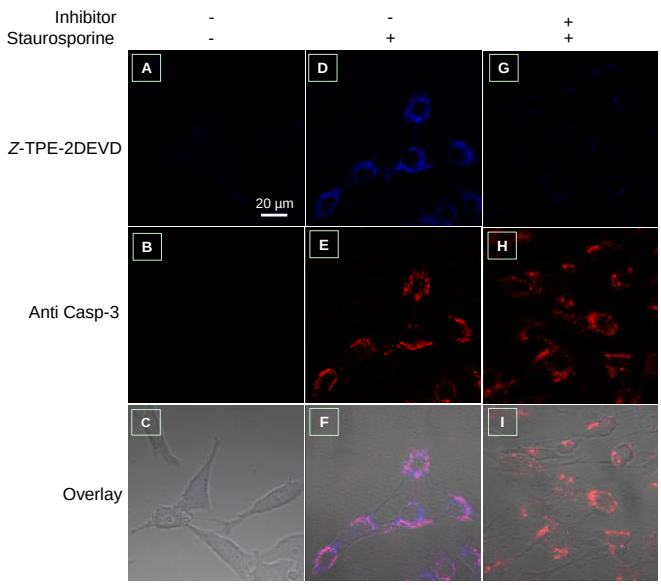

Fig. 7 CLSM images of normal MCF-7 cells treated with *Z*-TPE-2DEVD (A−C); apoptotic MCF-7 cells treated with *Z*-TPE-2DEVD (D−F), apoptotic MCF-7 cells treated with *Z*-TPE-2DEVD, inhibitor (10 μM), and caspase-3 antibody (G−I). Staurosporine (STS, 1 μM) was used to induce cell apoptosis. Blue: probe fluorescence; red: immunofluorescence signal generated from anti-caspase-3 primary antibody and a Texas Red-labeled secondary antibody. The signals were collected using DAPI and Texas Red filters for blue and red emissions, respectively. All images share the same scale bar (20 μm).

competed away when the cells are pre-treated with the inhibitor *Z*-DEVD-FMK (Fig. 7). These results indicate that the probe is specific for cell apoptosis imaging.

Conclusions

In conclusion, a light-up probe for caspase-3 detection was designed and synthesized by dual-functionalization of an AIE fluorogen with DEVD peptides. The *E*/*Z* isomers of the probe were successfully separated and duly characterized. Molecular docking simulations reveal that *E*-TPE-2DEVD is more efficient in binding with caspase-3 that leads to accelerated reactivity as compared to *Z*-TPE-2DEVD. However, the *Z*-TPE-2DEVD exhibited a better light-up response than its *E*-counterpart due to higher brightness of the cleaved product *Z*-TPE-2A. The *Z*-TPE-2DEVD probe has demonstrated excellent selectivity towards caspase with a high signal-to-background ratio of ~258. The probe was effective for live cell imaging of caspase-3 activation, indicating its potential application for apoptosis monitoring. This study not only presents a facile strategy for caspase detection, but also aids in development of effective biological probes through deliberate design of molecular structures, especially those entail stereoisomers.

Acknowledgements

We thank the Singapore National Research Foundation (R-279-000-390-281), the SMART (R279-000-378-592), Singapore Ministry of Defence (R279-000-340-232), the Research Grants Council of Hong Kong (HKUST2/CRF/10 and N_HKUST620/11), Guangdong Innovative Research Team Program (201101C0105067115) and the Institute of Materials Research and Engineering of Singapore (IMRE/12-8P1103).

Notes and references

[a]Department of Chemical and Biomolecular Engineering, 4 Engineering Drive 4, National University of Singapore, Singapore 117585
[b]Department of Chemistry, Division of Biomedical Engineering and Institute of Molecular Functional Materials, The Hong Kong University of Science and Technology, Clear Water Bay, Kowloon, Hong Kong, China
[c]Institute of Materials Research and Engineering, 3 Research Link, Singapore 117602
[d]SCUT–HKUST Joint Research Laboratory, Guangdong Innovative Research Team, State Key Laboratory of Luminescent Materials and Devices, South China University of Technology, Guangzhou 510640, China
Corresponding author: cheliub@nus.edu.sg; tangbenz@ust.hk

† Electronic Supplementary Information (ESI) available: ^{1}H and ^{13}C NMR spectra of *E*/*Z*-TPE-2N$_3$ Single crystal structure of *E*-TPE-2N$_3$, photophysical properties of isomers, molecular docking models of *E*-TPE-2DEVD. See DOI: 10.1039/b000000x/

‡ These authors contributed equally to this work.

1 A. Pandey, C. Webb, C. R. Soccol and C. Larroche, eds., *Enzyme Technology*, Springer, Delhi, 2006.
2 (a) A. A. Levin, L. J. Sturzenbecker, S. Kazmer, T. Bosakowski, C. Huselton, G. Allenby, J. Speck, C. ratzeisen, M. Rosenberger, A. Lovey and J. F. Grippo, *Nature*, 1992, **355**, 359; (b) G. Bronzetti, C. Bauer, C. Corsi, R. Del Carratore, A. Galli, R. Nieri, M. Paolini, E. Cundari, G. C. Forti and J. Crenshaw, *Teratogenesis, Carcinogenesis, and Mutagenesis*, 1984, **4**, 365; (c) S. Smith, E. Scarth and M. Sasada, eds., *Drugs in Anaesthesia and Intensive Care*, Oxford University Press, New York, 2011; (d) G. Georges, B. Norberg, G. Evrard and F. Durant, *Acta Cryst.*, 1989, **C45**, 454; (e) H. C. Harder, R. G. Smith and A. F. Leroy, *Cancer Res.*, 1976, **36**, 3821.
3 (a) M. Ueda, G. Yang, Y. Ishimaru, T. Itabashi, S. Tamura, H. Kiyota, S. Kuwahara, S. Inomata, M. Shoji and T. Sugai, *Biorg. Med. Chem.*, 2012, **20**, 5832; (b) R. N. Hanson, L. W. Herman, R. Fiaschi and E. Napolitano, *Steroids*, 1996, **61**, 718.
4 J. F. Kerr, A. H. Wyllie and A. R. Currie, *Br. J. Cancer*, 1972, **26**, 239.
5 Y. Otsuki, Z. Li and M.-A. Shibata, *Prog. Histochem. Cytochem.*, 2003, **38**, 275.
6 T. Satoh and R. C. Gupta, *Anticholinesterase Pesticides: Metabolism, Neurotoxicity, and Epidemiology*, John, Wiley & Sons, New Jersey & Canada, 2010.
7 T.-J. Fan, L.-H. Han, R.-S. Cong and J. Liang, *Acta Biochim. Biophys. Sinica*, 2005, **37**, 719.
8 A. G. Porter and R. U. Jänicke, *Cell Death Differ.*, 1999, **6**, 99.
9 (a) P. L. Bardet, G. Kolahgar, A. Mynett, I. Miguel-Aliaga, J. Briscoe, P. Meier and J. P. Vincent, *Proc. Nat. Acad. Sci. U.S.A.*, 2008, **105**, 13901; (b) S. L. Diamond, *Curr. Opin. Chem. Biol.*, 2007, **11**, 46; (c) B. Laxman, D. E. Hall, M. S. Bhojani, D. A. Hamstra, T. L. Chenevert, B. D. Ross and A. Rehemtulla, *Proc. Natl. Acad. Sci. U.S.A.*, 2002, **99**, 16551; (d) S. Lee, K. Y. Choi, H. Chung, J. H. Ryu, A. Lee, H. Koo, I.-C. Youn, J. H. Park, I.-S. Kim, S. Y. Kim, X.

Chen, S. Y. Jeong, I. C. Kwon, K. Kim and K. Choi, *Bioconjugate Chem.*, 2011, **22**, 125; (e) Z.-G. Li, K. Yang, Y.-A. Cao, G. Zheng, D.-P. Sun, C. Zhao and J. Yang, *Int. J. Mol. Sci.*, 2010, **11**, 1413; (f) S.-Y. Lin, N.-T. Chen, S.-P. Sun, J. C. Chang, Y.-C. Wang, C.-S. Yang and L.-W. Lo, *J. Am. Chem. Soc.*, 2010, **132**, 8309; (g) J. F. Lovell, M. W. Chan, Q. Qi, J. Chen and G. Zheng, *J. Am. Chem. Soc.*, 2011, **133**, 18580; (h) D. Maxwell, Q. Chang, X. Zhang, E. M. Barnett and D. Piwnica-Worms, *Bioconjugate Chem.*, 2009, **20**, 702; (i) P. Ray, A. De, M. Patel and S. S. Gambhir, *Clin. Cancer Res.*, 2008, **14**, 5801.

10 J. Luo, Z. Xie, J. W. Y. Lam, L. Cheng, H. Chen, C. Qiu, H. S. Kwok, X. Zhan, Y. Liu, D. Zhu and B. Z. Tang, *Chem. Commun.*, 2001, 1740.

11 R. B. Thompson, ed., *Fluorescence Sensors and Biosensors*, CRC Press, Boca Raton, 2005.

12 Y. Hong, J. W. Y. Lam and B. Z. Tang, *Chem. Commun.*, 2009, 4332.

13 (a) J.-P. Xu, Y. Fang, Z.-G. Song, J. Mei, L. Jia, A. Qin, J. Z. Sun, J. Ji and B. Z. Tang, *Analyst*, 2011, **136**, 2315; (b) M. Wang, D. Zhang, G. Zhang, Y. Tang, S. Wang and D. Zhu, *Anal. Chem.*, 2008, **80**, 6443; (c) M. Zhao, M. Wang, H. Liu, D. Liu, G. Zhang, D. Zhang and D. Zhu, *Langmuir*, 2008, **25**, 676; (d) M. Wang, X. Gu, G. Zhang, D. Zhang and D. Zhu, *Anal. Chem.*, 2009, **81**, 4444; (e) W. Xue, G. Zhang, D. Zhang and D. Zhu, *Org. Lett.*, 2010, **12**, 2274; (f) M. Wang, G. Zhang, D. Zhang, D. Zhu and B. Z. Tang, *J. Mater. Chem.*, 2010, **20**, 1858.

14 J. Dong, F. Abulwerdi, A. Baldridge, J. Kowalik, K. M. Solntsev and L. M. Tolbert, *J. Am. Chem. Soc.*, 2008, **130**, 14096.

15 H. Shi, R. T. K. Kwok, J. Liu, B. Xing, B. Z. Tang and B. Liu, *J. Am. Chem. Soc.*, 2012, **134**, 17972.

16 J. Wang, J. Mei, R. Hu, J. Z. Sun, A. Qin and B. Z. Tang, *J. Am. Chem. Soc.*, 2012, **134**, 9956.

17 A. Illanes, *Enzyme Biocatalysis: Principles and Applications*, Springer: New York, 2008.

18 A. Qin, J. W. Y. Lam, L. Tang, C. K. W. Jim, H. Zhao, J. Sun and B. Z. Tang, *Macromolecules*, 2009, **42**, 1421.

19 E. Conti, M. Uy, L. Leighton, G. Blobel and J. Kuriyan, *Cell*, 1998, **94**, 193.

For TOC only